

Strip Footing on Sand Overlying Soft Clay with Geotextile Interface

Rethaliya R. P* and Verma A. K**

Introduction

In practice, the bearing capacity of foundations on soft clay can be improved by placing a layer of compacted sand or gravel. The lack of detailed design information concerning the bearing capacity of such inhomogeneous soil profiles is due primarily to the difficulty in obtaining exact solutions. In recent years, approximate solutions have been presented for a number of commonly encountered inhomogeneous soil profiles in an attempt to provide acceptable design data, with methods such as that of Hanna & Meyerhof (1980) frequently cited for the case of a sand layer overlying soft clay.

The earliest attempt to calculate the bearing capacity of a strong layer overlying a weak layer was that of Terzaghi and Peck (1948). They assumed that the upper layer served principally to spread the footing load to a large area on the lower layer surface, hence reducing its intensity. The bearing capacity of a surface footing is given by,

$$q_u = q_c [1 + 2(H/B) \tan \alpha] \leq q_s \quad (1)$$

Where,

q_c is the ultimate bearing capacity of weak clay and q_s is the ultimate bearing capacity of strong sand layer.

Jacobsen et.al (1977) carried out a number of model tests using a buried circular footing in a sand layer overlying clay and attempted to improve the Terzaghi's analysis by assuming that the load spread through an inclination of $2/\beta$ vertical units per horizontal unit. The parameter β was calculated from model tests and depends upon the ratio of bearing capacity of sand layer alone to the bearing capacity of clay layer alone, that is bearing capacity ratio (q_s/q_c), the bearing capacity of a footing is then,

$$q_u = q_c (1 + \beta B/H)(1 + \beta B/L) + \gamma.D \leq q_s \quad (2)$$

* Lecturer, Applied Mechanics Department, BBIT, V.V.Nagar-388120. Gujarat.
E-Mail : rprethaliya2009@yahoo.in

** Professor and Head, Structural Engineering, BVM Eng. College, V. V.Nagar-388120.
E-Mail : akvbm@yahoo.co.in

where,

$$q_s = 0.5\gamma BN_\gamma \cdot S_\gamma + \gamma \cdot D \cdot N_q \cdot S_q \text{ and } \beta = 0.1125 + 0.0344 (q_s / q_c)$$

Both the above procedures are illustrated in Figure 1.

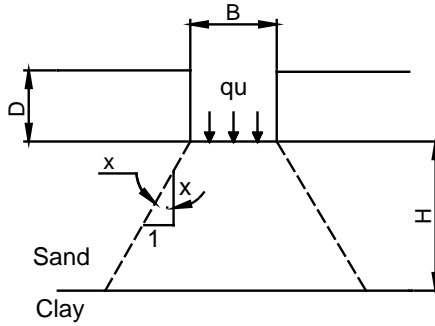


Fig. 1 Load Spreading Analysis for Sand Overlying Clay for $X=2$ (Terzaghi & Pexk-1948) and for $X=2/\beta$ (Jacobsen at al.-1977)

Hanna and Meyerhof (1980) developed a method supported by morel footing tests, which assumes that the forces acting on the vertical shear planes are the total passive earth pressure P_p inclined upwards at an angle δ to the horizontal. Since actual shear planes were observed to curve outwards from the footing, the mobilized angle of friction δ will be less than ϕ' for the sand. In addition, the mobilized passive earth pressure will decrease as the clay layer strength decreases. In order to facilitate a solution a coefficient of punching shear, K_s , is introduced.

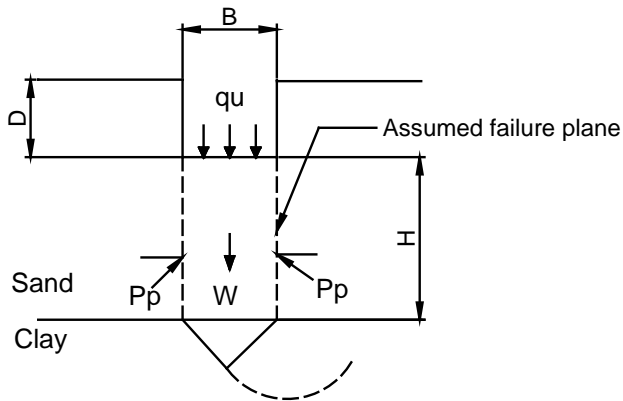


Fig. 2 Bearing Capacity Analysis for Sand Overlying Clay (Hanna & Meyerhof, 1980)

The solution for strip footing is given by,

$$q_u = q_b + \gamma H^2 (1 + 2D/H) K_s \cdot \tan \phi' / B - \gamma \cdot H < q_s \quad (3)$$

where, $q_b = q_c + \gamma(D + H)$

K_s is obtained from charts and its value depends on the mobilized angle of friction δ , the undrained shear strength of the clay c_u , the angle of friction of sand ϕ , and bearing capacity ratio q_s/q_c .

Shivashankar et al. (1993) studied the improvement in bearing capacity of footings resting on reinforced granular bed overlying soft clay, assuming a punching shear failure mechanism in the foundation soil. The improvement is attributed to three effects : (a) shear layer effect, (b) confinement effects due to the interaction between sand and reinforcement in the sand layer and (c) additional surcharge effects.

M.J.Kenny and Andrawes(1997) developed design charts from laboratory scale plane-strain bearing capacity tests under monotonic loading. In the analysis they considered load spreading angle 30° . They considered bearing capacity contribution from stress distribution through the upper sand layer and through membrane action.

Experimental Setup

The model tests for strip footings were conducted in a steel tank of effective size 1000mm (length) x 500mm (width) x 800mm (depth). The sides of the tank were braced with stiffeners to avoid lateral yielding during loading. The front wall of the test tank was fabricated from a 15mm thick Perspex glass sheet to facilitate the viewing of the failure mechanism as shown in Figure 3.

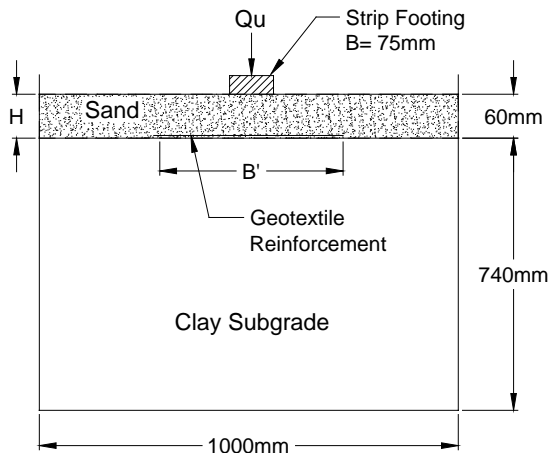


Fig. 3 Experimental Setup for Model Footing Tests

Mild steel plate of Strip shape with thickness 25mm was used as a model footing. The base of the model footing was made rough by cementing a thin layer of sand with a strong glue. The ends of the model footing were made as smooth as possible to reduce the friction during the tests.

Vertical loads were applied in stages at the centre of the model foundation setup, which is placed on the prepared soil bed and at the centre of the tank, through a hydraulic jack reacting against a self-straining loading frame. The hydraulic jack used was manually operated. The load and the corresponding footing settlements were measured by a proving ring and two dial gauges placed on each side of the footing.

Materials Used

Sand

Locally available uniformly graded river sand passing through 4.75mm I.S. Sieve and retained on 75 μ sieve was used for the model tests. The properties of the sand were determined according to IS code provisions and are presented in Table 1.

Table1 Index Properties of Sand

Index Property	Value
Uniformity Coefficient (Cu)	2.63
Coefficient of Curvature (Cc)	0.92
I.S. Soil Classification	SP
Specific Gravity	2.58
Maximum Dry Unit Weight (kN/m^3)	18.0
Minimum Dry Unit Weight (kN/m^3)	15.8
Dry Unit Weight (kN/m^3)	17.10
Relative Density (%)	62.20
Average Grain Size (D_{50}) mm	0.90
Effective Grain Size (D_{10}) mm	0.40

Clay

Locally available clayey soil was used in the investigation. The liquid limit and the plastic limit of the clayey soil are 38 % and 22 % respectively. The clay is classified as clay of intermediate compressibility (CI group) as per IS: 498-1970. The properties of the clay are given in Table 2.

Table 2 Properties of Clay

Property	Value
Liquid Limit (W_L)	38 %
Plastic Limit (W_P)	22 %
Plasticity Index (I_P)	16 %
Shrinkage Limit (W_S)	12 %
Specific Gravity	2.64
Free Swell Index	34.78 %
Undrained shear Strength (kN/m^2) at full saturation	12.0
Average saturated Unit Weight during Model tests (kN/m^3)	18.7
Average Moisture Content during Model Tests	33.35%
Gravel	0.0 %
Sand	4.6 %
Silt	58.0 %
Clay	37.4%
IS Classification	CI group

Reinforcement

The performance of reinforced layered soil system was studied using locally available woven geotextile, manufactured by Hi-Tech Specialty Fabrics (Exports) Pvt. Ltd., Vadodara. The properties of geotextile are presented in Table 3.

Table 3 Properties of Geotextile

Property	Value
Fiber	100 % Polypropylene
Structure	Woven Sheet
Type	HTSF-W3224
Equivalent opening size(mm)	$>0.15 <0.875$
Specific Gravity	0.91
Thickness in mm at (1 kPa)	0.60
Breaking Strength from 5cmx20cm strip	62 kN
(grip test) % Elongation at break	28 %

Soil Bed Preparation

The locally available clay was oven dried and pulverized, then randomly selected batches of dry clay were thoroughly mixed with predetermined amounts of water to achieve the desired water content. Based on the achievable dry density 14 kN/m^3 and water content 13.8 %, water content for full saturation condition was calculated as 33.55 %. [from $\gamma_d = G \cdot \gamma_w / (1 + e)$ and $e = wG / S_r$, $e = 0.886$]. Considering the loss of moisture during mixing and placing the soil in the tank, a 2 % surplus quantity of water was added to a weighed quantity of dry soil. The Clay layer with desired density was achieved by dropping clay lumps of about 2 kg mass freely from a height of 500mm. The drop height was selected by trial tests. Each layer was properly levelled by wooden tamper before placing next layer of clay lumps. The clay mass was completely covered with polythene sheet for 7 days for full saturation. The unit weight of clay sub-grade was obtained 18.7 kN/m^3 which was very close to its saturated density. Such a method of compaction and saturation yielded undrained cohesion value of 12.0 kPa obtained by unconfined compression tests.

The reinforcement, when used, was laid on the surface of the clay. The sand was placed on clay/reinforcement surface to the required depth. The air dried sand was allowed to fall freely from a funnel held at a constant height to obtain uniform density of fill. The height of fall required to obtain the desired density of sand was determined on the basis of trial tests. The model footing was placed centrally over the levelled sand bed.

Experimental Program

Bearing capacity tests were carried out for clay subgrade alone ($H/B=0$) and with and without the reinforcement layer for H/B ratios of 0.0, 0.2, 0.4, 0.6, 0.8, 1.0, 1.2, 1.4, and 1.6. In all the tests on reinforced soil, the width of reinforcement (B') was kept constant equal to $5.0B$.

Experimental results

Effect of depth of Reinforcement

The pressure-settlement relationships for unreinforced and reinforced sand overlying clay shown in Figure 4 are representative of the test program as a whole. It was observed that for the unreinforced soil system, an increase in the thickness of the sand layer resulted in an increase in the load carrying capacity and a corresponding reduction in settlement of the layered soil. Since there was no definite failure point observed in any of the load-settlement curves, the ultimate bearing capacity was determined by two tangents method. It is also observed that introduction of geotextile layer at the sand-clay interface further improves the performance of footing.

Figure 5 shows the variation of ultimate bearing pressure (q_u) versus H/B ratios for strip footing, with and without geotextile at the sand clay- interface. The bearing capacity of the layered system increases with the increase in thickness of sand layer up to a certain value of H/B . Beyond this value, there is no substantial improvement in the ultimate bearing capacity. The value of H/B at which maximum

bearing capacity is achieved is designated as $(H/B)_{cr}$. For strip footing the value of $(H/B)_{cr}$ are 0.8 and 1.4 for reinforced and unreinforced soil system respectively.

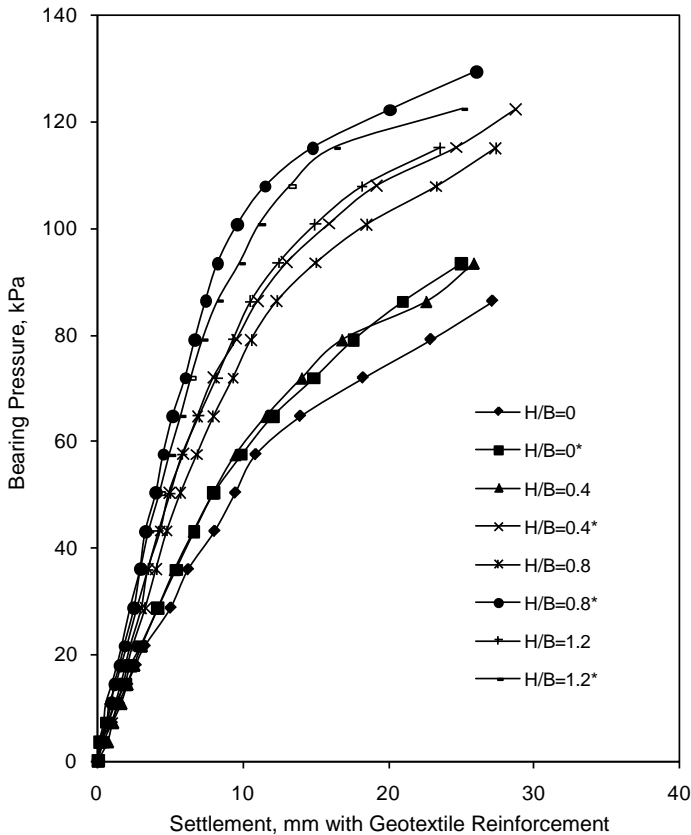


Fig. 4 Bearing Pressure -Settlement Relationship for Various H/B Ratios (Strip Footing)

The development of failure modes of the model tests was observed through the Perspex glass face during testing. The steady increase in bearing capacity of the unreinforced system can be attributed to the increase in the bearing resistance offered by the frictional granular soil as the fill thickness was increased. A thicker fill tends to spread the load over a wider area on the clay, thus increasing the ultimate bearing capacity of the footing. The observation of the failure surface at the end of the test showed that, at small H/B values the shear failure zones of soil developed below footing extended in to the soft clay sub-grade, thus resulting in low bearing capacities. With an increase in fill thickness, an increasing portion of the shear failure zone was developed within granular fill, thus accounting for the improvement in performance. For strip footing when thickness of the fill reached a value of $H/B = 1.4$, the entire shear failure surface was developed and contained within the granular fill layer, at which the bearing capacity reached the maximum value. Therefore, any further increase in fill thickness did not result in any additional improvement in bearing capacity, as the failure surface was always confined within the granular fill layer.

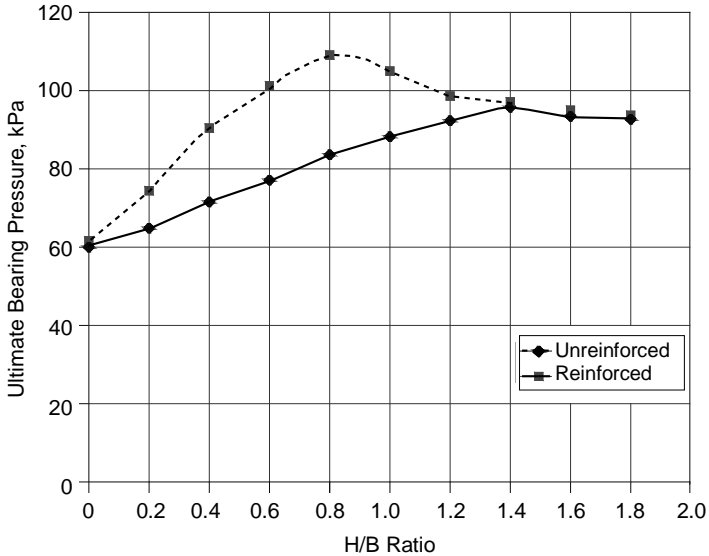


Fig. 5 Variation of q_u Vs H/B (Strip Footing)

In case of reinforcement at sand-clay interface, at small thickness of sand layer, large deflection developed on the geotextile directly underneath the footing. Since it is generally recognized that a large deflection on the geotextile would mobilize its membrane action and tensile resistance, such mechanisms act to modify the normal stress applied to the sub-grade by the combined action of tension in the reinforcement and membrane action in its curvature (Burd 1995). However, when the thickness of sand layer was increased beyond $(H/B)_{cr}=0.8$, a major portion of the shear failure zone of the soil was observed to develop above the reinforcement layer. This led to ineffective utilization of the membrane action and tensile capacity of the geotextile, and resulted in a gradual reduction of bearing capacity. Finally, when the thickness of sand layer was increased to a value of $(H/B) \geq 1.4$, no significant deflection was observed to develop on the reinforcement, and the shear failure zone of the soil was observed to develop well above the reinforcement layer. Therefore, at a fill thickness in excess of $H/B=1.4$, the system essentially behaved similar to the unreinforced system, thus the reinforced and unreinforced curves approached each other at $H/B \geq 1.4$. Hence, use of geotextile is totally ineffective, when H/B ratio exceeds 1.4, for strip footing.

Effect of Width of Reinforcement (B')

To study the effect of width of reinforcement on the performance of the layered soil, tests were conducted with varying widths of reinforcement in relation to footing width (B'/B ratio) for different shapes of footing. The depth of sand layer was maintained constant equal to $(H/B)_{cr}$ corresponding to a given footing shape as obtained earlier. In all the tests geotextile was used as reinforcement.

It was observed that there is a steady increase in ultimate bearing capacity with the increase in the width of reinforcement, up to $B'/B=5$ for strip footing, $B'/B=3.0$ for rectangular and square footing and $B'/D=3.0$ for circular footing. Further increase in the width of reinforcement in excess of critical B'/B or B'/D ratio, no noticeable improvement in the ultimate bearing capacity is observed. Thus, the results clearly indicate that there is an optimum value for the width of reinforcement at which the maximum bearing capacity can be derived, after which additional area of reinforcement becomes ineffective. This may be due to fact that below the footing there exists a zone of shearing deformation of soil and only that portion of reinforcement which lies within this zone, will have its tensile strength effectively mobilized. Some part of the reinforcement area beyond this zone serves as anchorage to provide pull-out resistance to the geotextile. Hence, an optimum width of reinforcement (B'), required will be equal to the sum of length of reinforcement within the shear zone underneath the footing and the length in the anchorage zones on both sides of footing. Any additional length of reinforcement beyond optimum value of B' , will be ineffective.

Effect of Size of Footing

In order to understand the effect of size of footing, model tests were carried out on both unreinforced and reinforced systems for three different sizes of square footing. The reliability of the model test results can be enhanced for field application if size effects are delineated. As mentioned earlier $(H/B)_{cr}$ and $(B'/B)_{cr}$ were maintained constant.

The bearing pressure- settlement relationships for all three footing sizes are shown in table-4. It is evident from the results that bearing capacity increases with increase in the size of footing, for both reinforced and unreinforced systems. The bearing capacity ratio (BCR) is observed to be nearly same for all the three sizes. This indicates that percentage improvement in bearing capacity as shown by small scale model footing tests on reinforced soil beds may not change much for prototype footings in the field.

Table 4 Effect of Size of Footing on Bearing Capacity

$(H/B)_{cr}=1.0$ for without reinf. $(H/B)_{cr}=0.6$ for with reinf. $B'/B=3.0$

Sr.No	Size of Square Footing	Settlement Ratio	Ultimate B.C. q_u kN/m ²		BCR
			without Reinf.	with Reinf.	
1.	150mm x 150mm	2.0	49.0	57.0	1.16
		4.0	72.0	90.0	1.25
		6.0	88.0	105.5	1.20
		8.0	99.0	114.5	1.16
		10.0	108.5	123.0	1.13
		12.0	117.0	129.0	1.10
		14.0	123.5	134.5	1.09
		16.0	128.0	141.0	1.10

Sr.No	Size of Square Footing	Settlement Ratio	Ultimate B.C. q_u kN/m ²		BCR
			without Reinf.	with Reinf.	
2.	100mm x 100mm	2.0	29.0	32.5	1.12
		4.0	51.5	59.0	1.15
		6.0	65.0	70.5	1.08
		8.0	72.5	82.0	1.13
		10.0	78.0	92.0	1.18
		12.0	82.0	98.0	1.20
		14.0	85.0	102.5	1.21
		16.0	87.5	106.0	1.21
3.	75mm x 75mm	2.0	15.0	19.0	1.26
		4.0	30.5	36.0	1.20
		6.0	42.0	52.5	1.25
		8.0	51.5	63.0	1.22
		10.0	60.0	72.0	1.20
		12.0	66.0	79.0	1.20
		14.0	70.5	85.0	1.21
		16.0	75.0	89.0	1.19

Effect of Shape of Footing

Four basic shapes of footings with their BCR are shown in Table 5. The type of reinforcement used was geotextile, while the values of $(H/B)_{cr}$ and $(B'/B)_{cr}$ were kept constant corresponding to their optimum values.

**Table 5 Effect of Shape of Footing on Ultimate Bearing Capacity
Type of Reinforcement - Geotextile**

Sr. No.	Type and Size of Footing mm	Size of Reinfo. mm	$(H/B)_{cr}$	$(B'/B)_{cr}$	Ultimate B.C. q_u kN/m ²		BCR
					Without Reinf.	With Reinf.	
1.	Strip Footing 75 x 500	375 x 500	0.8	5.0	83.5	109.0	1.31
2.	Rect. Footing 75 x 150	225 x 450	0.8	3.0	79.0	102.0	1.29
3.	Square Footing 150 x 150	450 x 450	0.6	3.0	72.0	102.5	1.42
4.	Circular Footing 450mmdia.	150mmdia.	0.6	3.0	66.0	91.0	1.38

It was observed that for a footing of given shape, the ultimate bearing capacity is considerably higher for a reinforced system, and at any given load, corresponding settlements are much smaller as compared to the unreinforced system. It is evident from the test results that percentage improvement in bearing

capacity (BCR) is almost same for all the four basic footing shapes. This is in contrast to behaviour in respect of unreinforced case. The shape factor which has different values depending upon the footing shape in case of unreinforced soil e.g. 0.5 for strip, 0.4 for square and 0.3 for circular (Lee and Manjunath, 1999) tends to a near constant value for footings on reinforced soil. This is due to a larger effective volume of soil that is involved in the reinforced case, which masks the shape effect.

The Reinforcement Mechanism

The reinforcement failure mechanism using geotextile at sand-clay interface under plane strain conditions as observed from model tests is illustrated in Figure 6. The wavy shape of deformed geotextile results from the incompressibility of sub-grade soil. The loading over width, B is transferred in X-Y plane through the sand fill and is distributed on the surface of geotextile over an increased width, B_r' with angle of load dispersion, α .

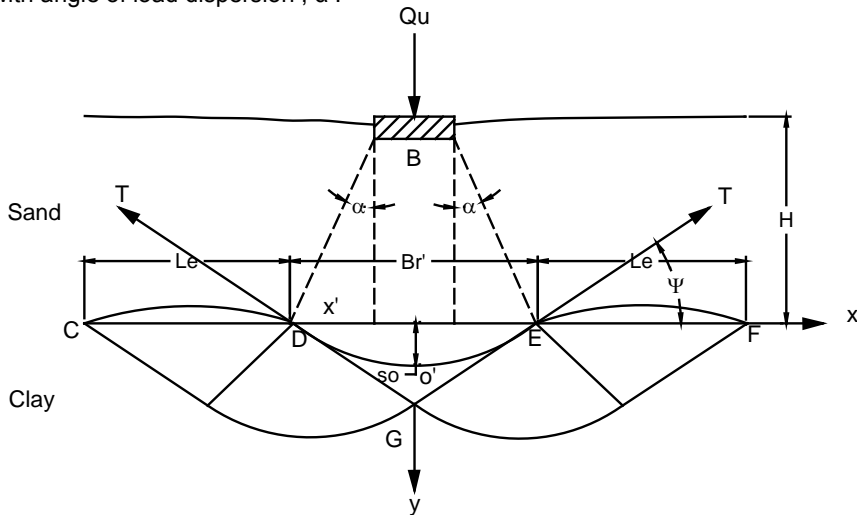


Fig. 6 Failure Mechanism for Reinforcement

The shape of deformed geotextile may be divided in to three parts, namely a central parabola between the points D and E on the initial plane of the geotextile with maximum settlement, S_o at its centre and two cubic parabolas with zero slopes at ends C and F on either side of the central parabola. A very little heave was observed during footing penetration.

When a granular bed of thickness H , of bulk density, γ_s and friction angle ϕ_s with reinforcement is provided over soft soil, the bearing capacity of the footing resting on this foundation medium is increased. Frictional forces developed between the soil and the reinforcement induces tensile strains in the reinforcement. The tensile strains developed provide the confining effect. This will induce additional shearing resistance along the vertical plane at the edge. Thus, the ultimate bearing capacity of the sand overlying soft clay with geotextile reinforcement at the sand-clay interface comprises of the contribution from stress distribution (q_d), contribution due to shear layer effect (q_s), and the contribution due to membrane action (q_m).

$$q_u = q_d + q_s + q_m \quad (4)$$

Contribution to bearing capacity from stress distribution (q_d)

From Figure 6 it can be seen that the contribution to the bearing capacity from stress distribution through the upper sand layer, q_d is:

$$q_d = q_c \cdot Br' / B \quad \text{kN/m}^2$$

$$q_d = c_u \cdot N_c \cdot Br' / B \quad (5)$$

where,

q_c = Bearing capacity of clay alone (It was taken from clay alone curve from Figure 4 at the same footing settlement). = $c_u \cdot N_c$

For bearing capacity factor N_c , a value of 5.14 is used in the computation (Giroud and Noiray-1981).

q_d = Contribution to the B.C. from stress distribution through the upper sand layer.

$$Br' = \text{Increased width of footing due to load spreading} = B + 2H \tan \alpha$$

Terzaghi and Peck (1948) assumed load spreading angle, $\alpha = 26.56^\circ$, M.J. Kenny (1998) considered, $\alpha = 30^\circ$. The value of α varies between 25° and 30° . In this analysis, the value of α was taken to 25° .

Contribution to Bearing Capacity due to Shear Layer Effect

Frictional forces developed between the granular soil and the reinforcement induces tensile strains in the reinforcement. The tensile strains developed provide the confining effect. This will induce additional shearing resistance along the vertical plane at the edge of footing, known as the shear layer effect. (Shivshankar et al., 1993). The concept is illustrated by Figure 7.

The passive earth pressure at depth H,

$$T = K_p \cdot \gamma \cdot s \cdot H$$

Total Earth Pressure = horizontal force acting at the base of the triangle

$$= 1/2 K_p \cdot \gamma \cdot s \cdot H^2$$

The shearing stresses that are developed along the vertical plane at the edge of the footing are given by,

$$\tau_f = 1/2 K_p \cdot \gamma \cdot s \cdot H^2 \cdot \tan \phi \text{ kN/m}$$

on one side of footing

q_s = Contribution to bearing capacity due to shear layer effect

$$= 2 \cdot \tau_f / B$$

$$= 2 \cdot K_p \cdot \gamma_s \cdot H^2 \cdot \tan \phi_s / 2B$$

$$= K_p \cdot \gamma_s \cdot H^2 \cdot \tan \phi_s / B \tag{6}$$

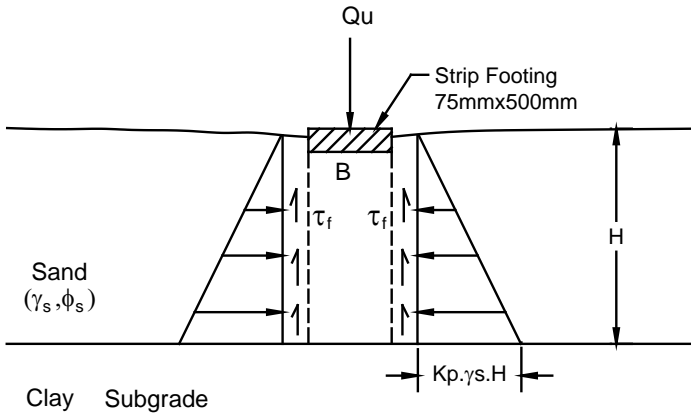


Fig. 7 Shear Layer Effect

Contribution to Bearing Capacity due to Membrane Action of Reinforcement (q_m)

Overburden pressure at E due to sand fill of depth H is equal to, $\gamma_s \cdot H$

Horizontal force developed in reinforcement per meter length,

$$t_r = \gamma_s \cdot H \cdot \mu_r = \gamma_s \cdot H \cdot \tan \phi_r \dots \text{kN/m}^2 \tag{7}$$

Friction force for length L_e ,

$$T_R = \gamma_s \cdot H \cdot \tan \phi_r \cdot LDR$$

Since, $LDR = 1$ for geosynthetics

$$T_R = \gamma_s \cdot H \cdot \tan \phi_r \cdot L_e \dots \text{kN/m} \tag{8}$$

From Figure 8, $\tau_f = T_R \cdot \tan \phi_s$ for one side of footing

q_m = Contribution to Bearing Capacity due to membrane action

$$= 2 \cdot \tau_f / B = 2 \cdot T_R \cdot \tan \phi_s / B = 2 \cdot \gamma_s \cdot H \cdot \tan \phi_r \cdot L_e \cdot \tan \phi_s / B \tag{9}$$

$$= 2 \cdot \gamma_s \cdot H / B \tan \phi_r \cdot L_e \cdot \tan \phi_s$$

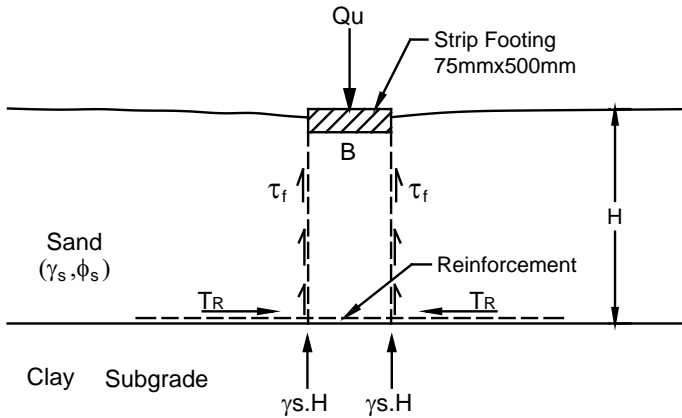


Fig. 8 Tension in Reinforcement (Membrane Action)

Now, we have

$$q_u = q_d + q_s + q_m$$

$$= c_u \cdot N_c \cdot Br' / B + K_p \cdot \gamma_s \cdot H^2 \cdot \tan \phi_s / B + 2 \cdot \gamma_s \cdot H / B \tan \phi_r \cdot L_e \cdot \tan \phi_s \quad (10)$$

Table 6 Comparison of Experimental and Predicted Bearing Capacities for Reinforced Sand Overlying clay

H/B	So at Ultimate Load(mm)	Br'/B	Predicted B.C. (kN/m ²)				Experimental B.C. (kN/m ²)
			q _d	q _s	q _m	q _u	q _{exp}
0.0	9.8	1.00	53.0	0.0	0.0	53.0	61.5
0.2	9.6	1.19	61.67	0.17	0.58	62.42	74.0
0.4	9.2	1.37	68.50	0.67	1.16	70.33	90.50
0.6	9.0	1.56	76.44	1.51	1.74	79.69	101.0
0.8	8.8	1.75	84.0	2.69	2.33	89.02	109.0
1.0	8.6	1.93	90.71	4.20	2.91	97.82	105.0
1.2	7.6	2.12	89.04	6.06	3.49	98.59	98.50
1.4	6.9	2.31	85.47	8.24	4.07	97.98	97.00

Effect of Surcharge

Surcharge load was applied on the two sides of strip footing in the form of brick layer and concrete cubes. At surcharge 3.6 kN/m², the bearing capacity contribution (q_m) was increased from 2.33 kN/m² to 10.49 kN/m² and the bearing capacity of footing was increased from 109kN/m² to 120 kN/m². The increase in

bearing capacity is attributed to the increase in the tension in the reinforcement due to application of the surcharge. The results are presented in table 7.

Considering the effect of surcharge, the equation (9) is modified as,

$$q_m = 2 \cdot (\gamma_s \cdot H + q) / B \tan \phi_r \cdot L_e > \tan \phi_s \quad (11)$$

where, q = surcharge pressure in kN/m^2

and equation (10) is modified as,

$$q_u = q_d + q_s + q_m$$

$$= c_u \cdot N_c \cdot Br / B + K_p \cdot \gamma_s \cdot H^2 \cdot \tan \phi_s / B + 2 \cdot (\gamma_s \cdot H + q) B \tan \phi_r \cdot L_e \cdot \tan \phi_s \quad (12)$$

Table 7 Effect of Surcharge on Bearing Capacity

Strip footing (H/B) \leq 0.8

Surcharge	q_m kN/m^2	Calculated q_u kN/m^2	Experimental q_u kN/m^2
Without Surcharge	2.33	89.02	109.0
Surcharge 1.529 kN/m^2 one brick layer	5.79	92.48	115.0
Surcharge 3.06 kN/m^2 two brick layer	9.27	95.96	117.0
Surcharge 3.60 kN/m^2 concrete block	10.49	97.18	120.0

Conclusions

Based on the experimental results and analysis presented above, the following conclusions can be drawn.

- > The model test results have shown that , while the provision of a layer of granular fill over the soft clay sub-grade leads to an increase in its load carrying capacity , the provision of a reinforcement layer at the sand clay-interface has resulted in an additional increase in bearing capacity and a decrease in settlement of the footing.
- > The optimum thickness of the sand layer which resulted in the ultimate bearing capacity of the geotextile reinforced foundation was found to be about 0.8 times the width of footing for strip and rectangular footings while 0.6 times the width of square and circular footings. On the other hand, for the unreinforced systems the optimum thickness of the sand layer was significantly higher.
- > The optimum width of the geotextile reinforcement for getting maximum improvement in bearing capacity of sand layer overlying soft clay was found

to be about $5.0B$, for strip footing and $3.0B$, for rectangular, square and circular footings. Any additional width of reinforcement beyond optimum value, will be ineffective.

- > The model tests conducted on footings of different sizes shows that the improvement in bearing capacity is same for all the three sizes. Hence, the relative improvement exhibited by reinforced soil bed with model footings may not change appreciably with prototype footings in the field.
- > The shape of footing does not affect the behavior of reinforced soil beds. This is in contrast to behavior in respect of unreinforced soil beds.
- > The contribution to bearing capacity due to membrane action can be further improved by applying additional surcharge on both the sides of footing by developing more tension in the reinforcement.
- > The mathematical modelling of strip footing on reinforced soil bed with geotextile reinforcement compares well with experimental results. The predicted bearing capacity values were found to be lower than the experimental values.

Notations

B	Width of Footing
B_r'	Increased Width of loading due to load spreading
α	Load Spreading Angle
B'	Width of reinforcement
L_e	Effective Length of Reinforcement
c_u	Undrained Cohesion of Clay
N_c	Bearing Capacity Factor for Cohesion
H	Depth of Sand Layer
BCR	Bearing Capacity Ratio
Q_u	Ultimate Load of Footing
q_u	Ultimate Bearing Capacity
q_c	Bearing Capacity of Clay alone
q_d	Contribution to B.C. by stress distribution through upper sand layer
q_s	Contribution to B.C. due to Shear layer Effect
q_m	Contribution to B.C. due to Membrane action
γ_s	Unit Weight of Sand
ϕ_s	Angle of friction for sand
ϕ_r	Angle of friction between sand and reinforcement
K_p	Coefficient of passive Earth pressure
LDR	Linear Density Ratio

References

- Burd H.J. (1995): 'Analysis of membrane action in reinforced unpaved roads', *Canadian Geotechnical Journal*, Vol.32, pp.946-956.
- Giroud J.P., Noiray L. (1981): 'Geotextile-reinforced unpaved road design', *Journal Geotech. Eng. Div., ASCE*, Vol.107, No.GT9, pp. 1233-1254.
- Hanna A.M. and Meyerhof G.G. (1980): 'Design Charts for Ultimate Bearing Capacity of Foundation on Sand Overlying Soft clay', *Canadian Geotechnical Journal*, Vol.17, pp.300-303.
- Jacobsen M., Christensen K. V. and Sorsen C. S. (1977): 'Penetration of thin sand layers', *Vag-och Vatten Byggarer*, Riksförbundet, Stockholm, Sweden, pp.23-25.
- Kenny M.J. (1998): 'The Bearing Capacity of a Reinforced Sand Layer Overlying a soft Clay Subgrade', *Sixth International Conference on Geosynthetics*, pp.901-904.
- Kenny M.J. and Andrawes K.Z. (1997): 'The Bearing Capacity of Footings on a Sand Overlying Soft Clay', *Geotechnique* 47, pp. 339-345.
- Lee K.M., Manjunath V.R. and Dewaikar D.M. (1999): 'Numerical and Model Studies of Strip Footing Supported by a Reinforced Granular Fill-Soft Soil System', *Canadian Geotechnical Journal*, Vol.36, pp.793-806.
- Shivshankar R., Madhav M.R. and Miura N. (1993): 'Reinforced Granular Beds Overlying Soft Clay', *Proc. 11th Southeast Asian Geotechnical Conference*, Singapore, pp. 409-414.
- Terzaghi K. and Peck R.B. (1948): *Soil Mechanics in Engineering Practice*, Wiley International, New York.